NBSIR 84-2983

Molecular Basis for Laser-Induced Vaporization of Refractory Materials

J. W. Hastie, D. W. Bonnell, and P. K. Schenck

U.S. DEPARTMENT OF COMMERCE
National Bureau of Standards
Center for Materials Science
Inorganic Materials Division
High Temperature Processes Group
Gaithersburg, MD 20899

December 1984

Annual Report

U.S. DEPARTMENT OF COMMERCE
NATIONAL BUREAU OF STANDARDS

NBSIR 84-2983

MOLECULAR BASIS FOR LASER-INDUCED VAPORIZATION OF REFRACTORY MATERIALS

J. W. Hastie, D. W. Bonnell, and P. K. Schenck

U.S. DEPARTMENT OF COMMERCE
National Bureau of Standards
Center for Materials Science
Inorganic Materials Division
High Temperature Processes Group
Gaithersburg, MD 20899

December 1984

Annual Report

U.S. DEPARTMENT OF COMMERCE, Malcolm Baldrige, *Secretary*
NATIONAL BUREAU OF STANDARDS, Ernest Ambler, *Director*

Molecular Basis for Laser-Induced Vaporization of Refractory Materials

J. W. Hastie, D. W. Bonnell, and P. K. Schenck
High Temperature Processes Group
Inorganic Materials Division
National Bureau of Standards
Gaithersburg, MD 20899

TABLE OF CONTENTS

Molecular Basis for Laser-Induced Vaporization of Refractory Materials

J. W. Hastie, D. W. Bonnell, and P. K. Schenck
High Temperature Processes Group
Inorganic Materials Division
Gaithersburg, MD 20899

1. Introduction and Summary

The interaction of high power lasers with refractory materials has been studied by a number of workers during the last two decades. Most of these studies have concentrated on the macroscopic, non-molecular processes such as: crater formation, material removal rate, and plume dynamics. The objective of the present study is to provide a molecular-level description of the vaporization processes, and to provide a fundamental link to smoke and aerosol formation. These processes are central to the interaction of high power lasers with graphitic or other refractory materials. This report describes the results of research carried out during FY84. The effort is divided into three interlinked subtasks, as follows:

- Subtask A: Laser Vaporization Kinetics of Carbon-Containing Refractories.

  Objective: To determine molecular specific mechanisms of laser-induced vaporization using high energy laser heating of surfaces, and time-resolved, high pressure sampling mass spectrometry of the vapor species produced.

- Subtask B: Mechanisms of Formation for Submicron Metal-Containing Particulates.

  Objective: To follow aerosol formation from expanding high temperature vapors in a vacuum environment. Particular emphasis is given to the mechanism for homogeneous nucleation which results from aggregation of molecular species to form cluster intermediates and macroscopic particulates.

o Subtask C: Ionization Processes.

Objective: To determine the influence of high temperature on molecular ionization processes, with emphasis on both partial and total electron-impact ionization cross-sections. A temperature dependence of these cross-sections would manifest itself in the electron impact fragmentation patterns of the C_n (n = 1 - 5) species, for instance, and could account for some of the disparate literature results on graphite vaporization thermodynamics.

Of these areas, subtask A is the primary effort, with subtask C providing important information regarding mass spectral interpretation. Subtask B deals with the link between the molecular-level initial vapor-forming process and the macroscopic process of aerosol formation. The principal research carried out under these three subtasks, during FY84, is summarized as follows with additional details given in Section 2.

For subtask A, a Laser-Induced Vaporization (LIV) facility has been constructed and tested. The apparatus consists of a 10 Hz, pulsed Nd/YAG laser coupled to a specially designed high pressure sampling mass spectrometer. In principle, the mass spectrometer can detect both charged and neutral species arising from the laser vaporization process. However, under the conditions of the present study, where laser-vapor plume interaction was avoided as far as possible, only neutral species were observed. Thus the ions referred to here are those resulting from electron impact ionization of molecular species in the mass spectrometer ion-source. Initial studies on an ultra-pure spectroscopic grade graphite sample, provided quantitative time-resolved mass spectral peaks of C_n (n = 1 - 5) singly charged positive molecular ions with excellent signal-to-noise ratios and reproducibility. The absolute and relative concentrations of the corresponding neutral species were consistent

with the establishment of local thermodynamic equilibrium at the sample "surface." The "surface" in these studies was actually slightly cratered by the focused laser beam, with a typical crater having dimensions of about 0.03 cm width and 0.01 cm depth. For minimum laser power (10 mJ) conditions, the surface temperature was determined indirectly from the mass spectral data to be 4100 ± 300 K at a total species pressure of one atmosphere (1 atm = 101,325 Pa). A beam-velocity analysis of the C_n species indicated an appreciable cooling effect (to 2500 K) in the vapor plume by an adiabatic expansion process. Additional studies are needed to identify the processes occuring at a smooth surface, in comparison with those resulting from the shallow craters formed under the present experimental conditions. Planned experiments include:

- o Traversing the sample surface between successive laser shots--to avoid crater-formation.
- o Use of a rod-like sample geometry, with a cross section dimension matching that of the hot-spot--to provide for a complete surface regression as opposed to cratering.
- o Data collection, at a fixed sample position, as a function of number of laser shots and, hence, crater size--to follow the transition between free (vaporization coefficient, $\alpha \leq 1$) and Knudsen-like (equilibrium, $\alpha \equiv 1$) vaporization conditions.

Based on these initial results, obtained with the 10 Hz Nd/YAG laser system, and also earlier tests with a CW CO_2 laser, a new laser has been selected (and procured by NBS) for permanent coupling with the mass spectrometric system. This 20 Hz Nd/YAG laser has recently been optically coupled with the mass spectrometer. However, delivery and installation of the

doubling crystals and the beam collimation telescopes, necessary to proper propagation of the beam, has been delayed (~ 6 months) by the vendor, and the new system is not expected to be fully operational until early in 1985.

Under subtask B, attempts to produce molecular clusters by non-equilibrium adiabatic expansion of NaCl, KCl, and C_n (n = 1 - 5) molecular species showed no evidence of clustering at source vapor pressures to one atmosphere. Apparently, higher pressures and longer expansion times (e.g., larger nozzles and lower expansion pressure-ratios) are needed to remove the appreciable excess energy produced in the initial aggregation process. It is also possible, though unlikely in the present case, that a small amount of clustering may remain undetected due to destruction of the clusters during the electron impact ionization process in the mass spectrometer. Additional studies are planned to determine the conditions needed for cluster formation and detection.

With regard to subtask C, we have found that the electron impact ionization cross-section (σ) can vary quite significantly with temperature, particularly for species exhibiting a large geometry change on ionization. Data obtained for the test cases, NaCl and KCl, exhibited large changes in σ (25:1) between high temperature (~ 1000 K) species and translationally cooled low temperature (~ 50 K) molecules. A quantitative potential energy curve model has been developed to account for this initially unexpected effect. The model has also been extended, on a qualitative basis, to allow for predictions of temperature dependent electron impact fragmentation with other high temperature species, including C_n (n = 1 - 5). Future studies will attempt to validate and improve the model.

2. Subtask A: Laser Vaporization Kinetics of Carbon-Containing Refractories --Results and Discussion

2.1 Apparatus and Experimental Approach

The basic apparatus, developed especially for this subtask, is shown schematically in figure 1. Note that the laser, molecular beam orifices, and mass spectrometer are configured to reduce the possibility of laser interaction with the portion of vapor plume directed toward the mass spectrometer. Such an interaction could lead to ionization and plasma effects not characteristic of the vaporization process, as noted in earlier studies, e.g., see Lincoln and Covington [1975]. The laser beam enters the first pumping stage of the Vertical High Pressure Sampling Mass Spectrometer (VHPMS) at right angles to the mass spectrometer beam line, as shown in figure 1.

The laser system basically consists of an externally mounted 10 Hz Nd/YAG laser (very recently upgraded to 20 Hz), operating at wavelengths from 1060 nm to 350 nm. To allow for ready visual alignment of the beam, the 532 nm doubled line of the laser fundamental was chosen as the working wavelength for the present studies. The laser pulse time used was about 7 nsec, which is negligible on the time scale of the vaporization process. This process required about 0.5-1 μsec for a 10 percent change on the leading edge of the ion intensity-versus-time signal profile. Earlier studies, such as those of Ohse, et al., [1979], have indicated the utility of short pulse time, high power lasers (e.g., Nd/YAG) for controlled surface vaporization studies. The laser beam was focused onto the sample by a 500 mm focal length lens, mounted on a movable stage. A spot size of 250 microns was used. The laser was operated near threshold and adjusted to deliver the same power for each pulse in a data-averaging series.

Figure 2 shows details of the VHPMS vacuum system. The viewpoint (normal to the page) is that of the entering laser beam. For the present study, the chopper, in stage III, has been anchored with an open aperture centered on the beam line. The blade apertures are much larger than the diameter of the collimated beam. In the vacuum system, the mean free path of gas is always much greater than the local geometry. In the sample region, the pumping speed is calculated to be at least 1500 1/s. This pump conductance has been confirmed by pressure measurements at known gas loads. Although the vaporization time scale is too short for the pressure gauges to respond, the local pressure outside the gas-dynamic shock boundaries should be in the molecular flow regime, with a mean free path length much greater than the distance from sample to the skimmer orifice. Thus we can eliminate from consideration any possible perturbation of the plume sample by post-expansion collisions.

The sample was mounted on a stainless steel bar. Graphite samples were taken from a rod of spectroscopic grade graphite selected by the NBS Analytical Chemistry Division for spectrographic analyses on the basis of its freedom from contaminants. The hydrogen content is unknown but probably insignificant, although weak mass spectrometric signals were observed corresponding to C_2H_2 and other low hydrogen-content gas species. Possible hydrocarbon contributions to the C_n^+ (n = 1 - 5) ion signals are estimated to be less than a few percent and can be neglected. Sample preparation consisted of parting-off a short section of 1/4 inch (~ 6.4 mm) rod, and milling a flat of the desired angle using carefully cleaned steel cutting tools. The angle between sample surface and mount (or laser beam, see figure 1) was chosen as 15 degrees for the data reported here. This geometry represented a compromise between the laser-entrance and mass spectrometer sampling angles.

The reduced mass flux for the slightly off-axis sampling was not expected to be significant, as shown by the earlier study of Covington et al., [1977]. From post-run examination of deposit patterns around vacuum chamber apertures, the vaporization process was shown to be approximately independent of the laser incidence angle and the plume was normal to the surface to within a few (~ ± 5) degrees for sample-surface to mount angles from 45 to 15 degrees.

In a typical laser-induced vaporization experiment, a 7 nsec 10 mJ laser pulse was focused at the sample surface by a 500 mm focal length f/10 lens which produced a spot size of 250 microns. The 20 J/cm^2 of deposited energy is converted into thermal excitation at the surface and penetrates to a depth of only a few tens of atomic diameters. Rapid vaporization occurs, leading at peak-temperature to the formation of a gas-dynamically stabilized plume which yields a molecular beam. The beam is collimated by three circular differentially pumped apertures, and travels a distance of 26 cm between the sample and ion chamber. Each aperture is sized to just allow clear passage of the beam through the 4.8 mm diameter entrance aperture of the mass filter ion source, and also through the larger ion source exit. Species are ionized by electron impact at adjustable voltages, and mass analyzed by a quadrupole mass filter. These filtered ions are then collected and amplified by an electron multiplier. The signals are averaged, with 0.5 usec/channel dwell time, with the sweep synchronized by a trigger generated from the onset of each laser pulse. This data collection process gives a time-resolved intensity-profile of an individual mass peak. Sufficient signal time-sweeps are collected (typically between 100 and 1000) to provide reasonably good statistics in the leading edge and peak centroid area. The process is repeated for each individual mass peak. It was observed that,

dependent on laser beam to surface angle, the initial signal intensity would decay during the first few tens of pulses and then stabilize at a value about half that produced by the initial pulse. For this reason, each series of intensity-time profiles (for individual masses) were collected after a pre-conditioning period, and successive series were taken from a new spot on the surface. To check the amount of signal loss, with the number of laser shots, the major peak (C_3) was sampled both at the beginning and end of a series.

2.2 Results:

Figures 3-5 show time-resolved, averaged intensity-profiles for the 36 (C_3^+), 12 (C_1^+), and 24 (C_2^+) amu ions, respectively. Similar data were collected for the ions C_4^+ and C_5^+. As has been noted in previous studies, during initial heating hydrocarbon impurities are released from even high purity graphite (e.g., see Zavitsanos and Carlson, [1973]). In the present study, this effect was observed primarily in the form of C_2H^+ (25 amu), $C_2H_2^+$ (26 amu), and $C_4H_2^+$ (50 amu) mass spectral ions during the initial first few laser shots onto a given surface position. These signals tended to vanish more rapidly than those for the C_n species, suggesting the presence of surface hydrocarbon contamination. Of particular note was the long time delay for the 26 amu (C_2H_2) species, as compared with the C_n ions. A similar effect may be noted in the results of Lincoln [1969]. For comparison, both our data and Lincoln's show a time difference between 26 and 36 amu of 150 to 200 μ sec. We attribute this time delay either to the $C_2H_2^+$ arising from electron impact fragmentation of a heavier polyacetylene precursor (the delay implies a species of 110 ± 15 amu) or, to a reaction time such as diffusion in the substrate. The 57 amu ($C_4H_9^+$) ion showed an even larger delay time and the intensity-time profile was exeptionally wide.

The intensity-time profiles from C_n are quite similar to those observed in analogous measurements by Olstad and Olander [1975] for Fe_n species. These authors provide a theoretical analysis of the atom density pulses in terms of an equilibrium vaporization model with known laser pulse energy-time profiles. A similar analysis should be possible for the C_n system.

Table 1 gives results from two runs at widely differing ionizing electron energy. The validity of the assignment of ions to neutral precursors is borne out by the insignificant changes in ion ratios from 26 eV to 96 eV ionizing electron energy. Ion intensities, proportional to neutral gas concentrations, were computed from the intensity-time profiles using, (1) the peak maximum at peak centroid, and (2) the integrated peak intensity. Both approaches gave consistant results which were almost independent of ionizing energy. However, the peak maximum results indicated the presence either of a slight excess of atomic-carbon, or of an unknown sampling artifact which affects only the lowest mass C_n species (see also Section 2.3).

The results of Table 1 may be interpreted to indicate that the graphite species vaporization coefficients appear to be very close to unity, contrary to the results of earlier work. This observation may result from the effect of signal-averaging several hundred vaporization events from a crater which could serve as a crude Knudsen cell. Other significant causes of data differences between this and earlier work may arise from our avoidance of a significant laser/plume interaction and the use of very short laser pulses to reduce perturbation of the gas-dynamic process. Also, as the present study was performed off the central plume axis, it is possible that if

non-equilibrium effects occurred only along the perpendicular axis they would not have been observed in the present work. As the plume is highly forward-peaked in the perpendicular direction this possibility needs further study.

2.3 Temperature Determination

For these initial studies, several indirect methods have been used to derive an estimate of the temperature (T_o) of the laser heated spot. Application of potentially more accurate optical pyrometric methods have been deferred due to uncertain emissivity data and the difficulty of accounting for plume contributions to the emission signals. Under the laser pulse conditions used, it is likely that only the surface layer (a few wavelengths, i.e., ~ 2000 to 5000 nm) is heated and the total extent of vaporization is confined to an area nearly equal to that of the laser spot [Hall, 1984]. The initial tests used a laser spot intensity profile which is roughly "donut-shaped." The effect of such a spot geometry, relative to a gaussian profile, should be to level-out the temperature profile of the heated area.

2.3.1 Beam Velocity Analysis

The time-of-arrival, Δt, of the beam-species may be used to obtain the plume temperature. Regardless of the exact model of the vaporization and beam-forming process, if a collection of gas molecules are in thermal equilibrium their velocity function is proportional to $(T_o/M)^{1/2}$, where M is the individual species molecular weight. As Δt is inversely proportional to velocity, a linear plot of Δt versus $(M)^{1/2}$ is indicative of thermal equilibrium. Figure 6 shows that the various C_n species exhibit such behavior, although the slope appears to be slightly dependent on electron energy, for reasons yet to be determined. Using the assumption of the equipartition of translational energy, one has

$$Mv^2/2 = 3kT/2, \qquad (2.1)$$

where v is the most probable velocity, i.e., the peak of the thermal velocity distribution, and T is the beam temperature ($<T_o$). Because the peak of the observed ion intensity-time-profile is considered to be caused by cooling of the sample, the arrival times were selected at the half-height position of the leading edge of the profile. Correlating this time with the most probable velocity yields the time-of-arrival function

$$\Delta t = (d/3kT)^{1/2} \cdot M^{1/2} \qquad (2.2)$$

where d is the flight distance, 26 cm. Note, in figure 6, that the zero mass intercept, a measure of the inherent delay in the quadrupole filter, is quite small. From these arguments, and the slope of the 100 eV curve of figure 6, we obtain a beam temperature estimate of 2500 ± 300 K. This temperature is much lower than is reasonable for the degree of vaporization observed and may be taken as evidence of expansion-cooling, followed by translational equilibration as the vapor species pass through a shock-front stagnation zone. Ohse, et al., [1979] have noted that for free vaporization from a surface, gas-dynamic models predict a rapid temperature drop to the sonic point such that $T \sim 2T_o/3$. This prediction, together with the above velocity model, suggests a pre-expansion temperature ($\sim T_o$) of 3800 ± 300 K, which is quite consistent with the thermodynamic arguments given below. Although this temperature analysis is not yet rigorous, our experimental results (not given here) for the thermochemically more-established BN system provide excellent

confirmation, as we obtain 4000 ± 300 K by comparing the C_2^+ arrival time relative to that for B^+ at T_o = 2900 K (see table 2). Other supporting arguments are also summarized in table 2.

2.3.2 Species Intensity Analysis

The time-of-arrival evidence for thermal equilibrium suggests that the "known" C_n species distribution with temperature can be used to derive the sample temperature (T_o) from the measured species concentration ratios. Also, the beam-formation process is quite similar to that for more usual supersonic expansions, where the beam composition represents a "frozen equilibrium" and corresponds to the pre-expansion temperature/pressure conditions [Bonnell and Hastie, 1979]. The high pumping speed of the vacuum system used for the present studies, and the pulsed nature of the gas evolution process, further ensures high expansion ratios and "frozen equilibrium" compositions in the gas-dynamic process.

Values of "known" C_n species concentration ratios were calculated as a function of temperature using the JANAF [1971] thermochemical tables. While other sources of thermodynamic data exist (see discussion in section 2.4), these tables still provide the most widely accepted critically evaluated thermodynamic functions for C_n species. Table 1 gives temperatures calculated from the listed C_n/C_3 ratio data. Note that although the temperature from the C_1/C_3 ratio fortuitously agrees with the post-expansion temperature (time-of-arrival data), such a temperature is unrealistically low for the observed species pressures. The corresponding ratios for the C_4 and C_5 species yield temperatures that are more consistent with those expected and also with those indicated by the above beam velocity analysis.

The anomalous low temperature result could be interpreted as being due to an apparent excess of C_1. Arguments for and against additional sources of C_1^+ include:

- o Electron impact fragmentation of higher mass C_n species or contaminants such as CO or hydrocarbons. In this connection, it should be noted that the literature data were usually obtained at lower electron energies than for the present study. However, the present results are consistent with the lower eV data of Berkowitz and Chupka [1964] and Drowart, et al., [1959].
- o A compelling argument against significant fragmentation in the present study is the time-of-arrival result which indicates that C_1^+ arises primarily from a 12 amu neutral, i.e., C_1.
- o Analysis of the C_n^+ ion-stabilities (bond dissociation energies) indicates no loss of stability on ionization of C_n; hence no major fragmentation effect is likely.
- o The constancy of ion-ratios over the range 26 to 96 eV is consistent with an absence of fragmentation and the existence of a single ion-precursor for all ions.
- o The C_1^+ appearance potential curve indicates C_1 as the major precursor.
- o From the C_1^+ ion intensity, the carbon-atom pressure (P_C) is calculated to be equal that obtained from JANAF [1971]. For this calculation k_C, the mass spectrometer ion intensity-partial pressure proportionality constant, was obtained from our established boron ion intensity data (not given here).

Wachi and Gilmartin [1970] found that C_1/C_n decreased with time, and also depended on the sample preparation and surface morphology. Also, considerable literature controversy exists concerning the entropy and hence absolute partial pressure of C_3. Thus, the use of observed C_1/C_3 ratios together with JANAF [1971] calculated ratios to infer temperatures, etc., seems risky. In this connection, literature more recent than JANAF [1971], as reviewed by Meyer and Lynch [1973], indicates C_1/C_3 < JANAF, with C_3 being more significant than JANAF; e.g., at 4000 K, with pressures indicated in atm,

C_1/C_3 (JANAF) = $(7.9 \times 10^{-2})/(5.0 \times 10^{-1})$ = 0.16, whereas

C_1/C_3 (M & L) = $(7.9 \times 10^{-2})/(1.2)$ = 0.066

i.e., JANAF is higher by a factor of 0.16/0.066 = 2.4,

i.e., C_3 (M&L) = 2.4 x JANAF.

This difference is comparable with the uncertainty in cross sections used to translate ion intensity to partial pressure data. However, use of the Meyer and Lynch [1973] or Meyer, et al., [1973] data and our C_1/C_3 results gives an even lower T_o than the JANAF value of 2600 K, which is impossible. Hence the C_1^+ data do not appear to have thermodynamic significance for C_1 concentration measurement.

Another, less-likely, argument as to why C_1/C_3 gives a lower T_o than C_n/C_3 ($n > 1$) is based on the higher sublimation enthalpies for C_n($n > 1$), as compared with C_1. This means that C_1 becomes a relatively more important species at lower temperatures and, as the hot spot cools, C_1 could become more significant than C_n ($n > 1$). However, this would require T_o, as calculated from the crater size, to be less than from the C_n/C_3 ratio data.

No systematic crater size data have been obtained to test this hypothesis. However, for our analogous study of BN (results not given here), the crater size measurements gave a high value for T_o. This explanation would also require our observation of B/B_2 to yield a lower T_o which was not the case.

For the case of the C_2/C_3 ratio (see table 1), if the relative ionization cross-sections were 1/1.5, which is quite reasonable based on empirical trends in other systems, the calculated temperature would be 4200 K, in agreement with the values obtained using the C_4 and C_5 species. This cross-section ratio agrees favorably with the estimate of 1/1.23 given by Meyer and Lynch [1973]. The higher polymeric C_n species should have cross-section ratios close to unity, which we have assumed in the present analysis.

2.4 Literature Studies of Laser-Induced Vaporization of Graphite

Since the JANAF evaluation, dated December, 1969 [in JANAF, 1971], a number of studies of the graphite vaporization system have been reported over the period 1968 to 1983. Analysis of the results of these studies indicates that the equilibrium distribution of various carbon species at temperatures greater than 2800 K is still uncertain.

2.4.1 Literature Survey for the Period 1968-1983

o Zavitsanos [1968]

Zavitsanos [1968] carried out laser vaporization mass spectrometric studies using conditions similar to those of the present work. However, only the C_1/C_3 ion intensity ratios are comparable between the two studies, as shown in table 3. The crater dimensions observed by Zavitsanos [1968], and those found in the present study, are notably similar for various graphite-types at 4100 K with similar laser energy conditions.

o Clarke and Fox [1969]

The vaporization data from graphite filaments at temperatures to 3400 K were analyzed in terms of C_2 as the principal species with a vaporization coefficient, $\alpha = 1$. For this analysis, the JANAF $\Delta H_{rn}(298)$ (i.e., for $2C(s) = C_2$) was assumed to be correct and equal to 832.6 kJ/mol. Assumptions of C_1, C_2, and C_3 as the principal species with $\alpha = 1$, or with the Thorn and Winslow [1957] α values, do not fit the data. Later workers have apparently not attempted to rationalize the results of Clarke and Fox [1969] with the prevailing viewpoint (including the present results) of C_3, rather than C_2, as the dominant species. These authors also cite all pertinent earlier literature work.

o Wachi and Gilmartin [1970]

These workers studied the free vaporization (Langmuir) behavior of various graphites using both double-focusing magnetic sector and time-of-flight mass spectrometric detection of the C_1 to C_5 species. A relatively low ionizing electron energy of 17 eV was used. Above 17.5 eV, the appearance potential curve for C_3 showed a pronounced upward curvature, indicating possible fragmentation of higher molecular weight species. Ion molecule reactions in the ion source were also suggested as a possible additional source of C_3^+. Apparent activation energies were basically in agreement with those reported earlier by Zavitsanos [1968]. No attempt to convert the ion intensity data to absolute species concentrations was made in this study. Thus, these results cast little light on the equilibrium thermodynamic vaporization behavior of the various C_n species. It is pertinent, however, to note the close similarity between the activation energies and equilibrium enthalpies (literature data) of vaporization. This similarity suggests local equilibrium conditions may be present under free

vaporization conditions for graphite. Another important observation from this study was the pronounced time-dependency of the relative ion intensities, with C_3^+ showing a strong increase, with time, relative to C_1^+ and C_2^+. This effect was tentatively attributed to changes in surface morphology and the suggested possible formation of an allotropic form of carbon.

o Milne et al. [1972]

Using Knudsen effusion mass spectrometry, these workers obtained relative ion intensity mass spectral data for C_1^+ - C_7^+ at temperatures to 3300 K at 17 eV electron energy. The ion ratios between C_1, C_2, C_3 and C_5 agree well with the extrapolated data of Drowart et al. [1959], and hence JANAF [1971]. The C_4 partial pressures were lower than those indicated by JANAF [1971] and the C_6 and C_7 values were lower than theoretical predictions, including those of Leider et al., [1973]. Useful second law data were obtained only for the relatively abundant C_3 and C_1 species. During initial heating, C_4 (48 amu) was anomalously high due to presence of a Ti impurity at the same amu. A comparison between the extrapolated results of Milne et al., [1972] and the present work is given in Table 4. Note that C_2/C_3 is the only ion ratio in agreement for the two studies.

The Milne et al., [1972] intensity-time profiles showed multiple peaks from each ion, which they attributed to possible ion trapping in the ion source. The positions and shapes for C_1^+, C_2^+ and C_3^+ suggested substantial C_3 fragmentation at 50 eV and none at 17 eV. There was also some indication of C_3^+ fragment-ion formation at the higher temperatures. The narrow C_3^+ peak shape was indicative of non-effusive expansion conditions. Note, however, that their pressures did not exceed ~ 10^{-3} atm for a 1/8 in. diameter cell orifice size and these conditions, while outside of molecular effusion, would not lead to significant gas-dynamic cooling.

o Zavitsanos and Carlson [1973]

Knudsen effusion mass spectrometry to 3000 K indicated good agreement with the JANAF [1971] C_1 - C_4 partial pressures. But the JANAF C_1 pressures were used to calibrate the pressure scale. These workers also used the newer C_3 thermodynamic functions of Strauss and Thiele [1967] but this did not improve the poor agreement between second and third law C_3 vaporization enthalpies. The possibility (also suggested by others) of a temperature-dependent C_3 ionization cross section was mentioned as a possible source of error with the second law enthalpy. Heavier species than C_4 were not significant in this study. This observation does not conflict with the analysis of Leider, et al., [1973] since they predict C_5 - C_7 as significant species at higher temperatures (> 4000 K) than the < 3000 K achieved by Zavitsanos and Carlson [1973]. The appearance potential data of these latter authors was considered evidence of negligible fragmentation at ionizing electron energies to 20 eV. However, the structure of their curves could also be interpreted to indicate fragmentation. More precise appearance potential measurements of C_3 [Wachi and Gilmartin, 1970] over pyrolytic graphite at 2788 K, showed a pronounced break at 17.5 eV, indicative (but not proof) of fragmentation of a higher polymer or other carbon-containing species. Extrapolation of these data to 26 eV suggests about 30 percent of C_3^+ could arise from fragmentation in the present studies.

o Meyer et al., [1973]

Pulse laser vaporization of pyrolytic graphite with mass spectrometric (time-of-flight) analysis indicated C_n integrated ion intensities (relative) of: C_1 (1.0), C_2 (1.3), and C_3 (18), at 18.6 eV, with higher n-species being negligible. Note that our corresponding values are: C_1 (1.0), C_2 (0.35), and C_3 (3.1), at 26 eV. Using estimated ionization cross sections and other

ion intensity conversion factors, the corresponding relative partial pressures for the Meyer et al., [1973] data are: C_1 (1.0), C_2 (0.32), and C_3 (35). Based on the Palmer and Shelef [1968] C_3/C_1 pressure ratio data, the temperature is indicated as 4500 K. Pulsed laser vaporization studies of graphite generally indicate surface temperatures in the range 4000 to 4500 K. From their analogous studies on TaC, where only C_1 and C_3 were significant, we can argue that the fragmentation, $C_1^+(C_3)$ or $C_2^+(C_3)$ is not a significant factor in the graphite mass spectra, at least to 18.6 eV.

Note that a significant difference between the Meyer et al., [1973] experiments and ours is their use of a single laser pulse and hence the need to consider vaporization coefficients in their conversion of ion intensities to partial pressures. Their intensity-time results are similar to ours and do not show the anomalous secondary peaks characteristic of the Milne et al., [1972] observations. However, their laser-plume geometry was coaxial, giving rise to possible laser perturbation of the plume species.

Hydrocarbon species noted by Meyer et al., [1973] over pyrolytic graphite included, C_2H_2, C_4H_2, and C_6H_2, in addition to H_2 and CO; C_2H_2 and CO were also noted over TaC.

o Meyer and Lynch [1973]

Their analysis of literature results is closer to that of Palmer and Shelef [1968], and also of Zavitsanos [1968] and Leider et al., [1973] than that of JANAF [1971]. The main result is that the C_3 partial pressures are predicted to be about three times greater than for the JANAF [1971] data. At temperatures in the region of 4000 K, the following differences are found between the Meyer and Lynch [1973] and JANAF [1971] evaluations:

$$\frac{C_1/C_3\ (ML)}{C_1/C_3\ (JANAF)} = 0.309 \qquad \frac{C_2/C_3\ (ML)}{C_2/C_3\ (JANAF)} = 1.06$$

$$\frac{C_4/C_3\ (ML)}{C_4/C_3\ (JANAF)} = 2.54 \qquad \frac{C_5/C_3\ (ML)}{C_5/C_3\ (JANAF)} = 2.35.$$

Table 5 gives a comparison of temperatures calculated using the ion intensities of the present work together with the Meyer and Lynch [1973] and JANAF [1971] partial pressure ratios. Note that the comparison using the JANAF data gives the more realistic temperatures.

o Lundell and Dickey [1977]

The graphite rate-of-mass-loss data of Lundell and Dickey [1977] agree well with JANAF [1971] provided unit vaporization coefficients are assumed for the temperature range of 4000 - 4500 K. Under the CW -CO_2 laser heating conditions used, the vapor plume was supersonic. Temperatures were determined by pyrometry of the surface using an estimated emissivity. This is one of the few graphite vaporization studies where controllable CW laser radiation was used and direct surface temperature measurements were made.

o Covington et al., [1977]

These workers have analyzed the gas-dynamic behavior of free-jet expansions from laser-vaporized carbon surfaces at temperatures to 4500 K. Their results are consistent with the JANAF [1971] tables, indicating equilibrium conditions and a species-averaged vaporization coefficient of 0.9 and an emissivity of 0.9. The data agreement with JANAF [1971] assumes C_1, C_2 and C_3 as the major species with the latter predominant. These workers also concluded that the vaporization process was independent of microscopic surface roughness.

o Gupta and Gingerich [1979]

These workers report Knudsen effusion data for C_1, C_2, and C_3 at temperatures to 2700 K. For the third law enthalpies, fair agreement with JANAF [1971] was obtained for C_1 and C_2; for C_3, $\Delta H_{atom\ (298)} = 1313 \pm 6.6$ kJ/mol, as compared with the JANAF [1971] value of 1321 ± 21 kJ/mol.

o Wulfson et al.,[1980]

These workers determined a maximum laser plume temperature of 3600 ± 300 K from the CN-impurity vibrational temperature for a pulsed laser graphite vapor plume. We believe that the conditions used would have yielded a total carbon-species pressure of about an atmosphere, similar to the present work.

o Lundell [1982]

From a review of earlier work, Lundell [1982] concluded that at relatively low temperatures (1400 to 2400 K) the vaporization coefficients are not well known but are considerably less than unity and differ between the various C_n species. At higher temperatures (3500 to 4500 K), the vaporization coefficients approach unity. Note that for the best available vaporization coefficient estimates and the JANAF [1971] data, C_1 is predicted to be the predominant species at the lower temperature range and C_3 at the higher range, with C_7 or other higher molecular weight species becoming significant above the boiling point.

o Baker et al., [1983]

The recent work of Baker et al., [1983], using similar methodology as for the study of Covington et al., [1977], provides an alternative analysis to that of Lundell [1982]. The results differed significantly from JANAF [1971] and were more consistent with the re-evaluation of Leider, et al., [1973]. However, the analysis depends to some extent on assumed emissivity,

species distribution, and vaporization coefficient behavior. Their analysis indicates an average α = 0.4 - 0.7, based on JANAF [1971], but that extrapolating to the melting point would require $\alpha > 1$, which is the primary basis for disagreement with JANAF. However, the linearity of the temperature-pressure extrapolation process is by no means assured. Comparison with the Livermore thermochemical tables [Leider, et al., 1973] indicates α = 0.2 - 0.6 over the data range and ~ 0.8 at the melting point. Based on the physical reasonableness of α approaching unity at the melting point, these authors preferred the Livermore to the JANAF analysis. The differences in Livermore and JANAF pressures are primarily only significant at temperatures higher than about 4200 K, which is the region most dependent on extrapolations and spectroscopically-based thermodynamic functions. The results of Baker et al., [1983] suggest α to be strongly temperature dependent. In this connection, it is pertinent to note that their carbon surface morphologies were relatively flat, as opposed to the cratered condition produced in the present studies.

2.4.2 Literature Summary, for the Period 1968-1983

Clarke and Fox [1969]

- o Indirect evidence of C_2 as the major species and α = 1 (3400 K).

Wachi and Gilmartin [1970]

- o Relative intensities of C_n^+ (n = 1 to 5) strongly dependent on time and sample form.
- o Possible evidence for C_3^+ fragment ion formation or ion-molecule reactions in the ion source above 17.6 eV.
- o Data insufficient to compare with JANAF [1971].

Milne et al., [1972]

- o Basically in agreement with JANAF [1971] (to 3300 K).
- o Time-of-arrival data suggests some fragmentation of C_3.

Meyer et al., [1973]

- o C_3/C_1 ion ratios are consistent with a laser plume temperature of 4500 K.
- o No evidence of C_1^+ or C_2^+ fragment ions from C_3 at 18.6 eV.

Meyer and Lynch [1973]

- o P_{C_3} ~ 3 X JANAF [1971]

Zavitsanos and Carlson [1973]

- o Knudsen mass spectrometry results to 3000 K, agree with JANAF [1971].

Lundell and Dickey [1977]

- o Results agree with JANAF [1971] at T = 4000-4500 K.
- o Conditions similar to the present study but mass-loss method used instead of mass spectrometry.

Covington et al., [1977]

- o Laser vapor-plume analysis to 4500 K.
- o α ~ 0.9.
- o C_3 is indirectly indicated the major species.
- o Results are consistent with JANAF [1971].

Wulfson et al., [1980]

- o Laser vapor-plume temperature 3600 ± 300 K.

Baker et al., [1983]

- o Data more consistent with analysis of Leider et al., [1973] than for JANAF [1971].
- o α = 0.2 - 0.6; ~ 1 at melting point
- o α strongly temperature dependent.
- o Data depart from JANAF [1971] mainly at T > 4200 K.
- o P total $\leq$ 2 X JANAF up to 4200 K, ~ 3 X [JANAF] at 4500 K.

2.4.3 Literature Summary, for the Pre-1968 Period

The JANAF [1971] evaluation is based on data available prior to 1968. An independent critical analysis of results from this period has also been made by Palmer and Shelef [1968], using theoretical C_3 entropy results not available to JANAF [1971].

The principal conclusions are:

- o $P_{total} \sim 10 \times P_{JANAF}$ (at T ~ 4000 K).
- o $T_{boiling} \sim 3850$ K vs. 4150 K for JANAF [1971].
- o The carbon-atom may be used as a reference point as its properties are well established.
- o Entropy of C_3 is about 21 J/mol·K greater than JANAF at [1971] 4000 K.

2.4.4 Conclusions From the Literature Survey

Despite recent suggestions to the contrary, the JANAF [1971] tables still appear to be the most consistent with the available data. However, a re-evaluation of all the thermodynamic functions is warranted as the JANAF [1971] data-consistency may result from offsetting errors, particularly for the C_3 species.

2.5 Carbon Vaporization from Carbides

For spacecraft survivability, under laser irradiation, the development of ablative coatings is a promising approach. An important coating requirement is the maximization of energy absorption, which implies minimizing the energy stored as chemical bonds in the vaporized protectant. In the case of carbon, the fact that C_3 is the predominant vapor species at high temperatures makes carbon a less favorable ablator than if carbon atoms were the preferred vaporizing species. Over pure carbon, it is thermodynamically unreasonable to significantly modify the vapor species distribution. However, with refractory metal carbides, the reduced thermodynamic activity of carbon species should favor release of lower molecular weight C_n-species,

in comparison with graphite. Carbides can also improve the refractory properties of ablative coatings. Tantalum carbide (TaC) is a promising ablation material and is a suitable test case for a detailed analysis of vaporization kinetics. A limited understanding of TaC vaporization processes is available from several earlier studies, described as follows.

Langmuir vaporization studies of refractory metal carbides, including those of Ta, Nb, Hf, Zr, and Ti have been reported by Fesenko and Bolgar [1969]. Vaporization rates increased in the above order, Ta to Ti. The data were also consistent with vaporization to metal plus atomic-carbon. However, this assignment may not be definitive owing to the non-molecular-specific approach used. At the highest temperature of 3373 K, the total pressure over the congruent vaporizing composition, $TaC_{0.71}$, was 4.5×10^{-5} atm. From this pressure, and the condition of congruency, we can compute the thermodynamic activity of C_3 as 1.56×10^{-3}. This reduced activity of C_3 in $TaC_{0.71}$, as compared with graphite (1.0 by definition), favors dissociation to C_1. At 3373 K the ratio $P_{C_1}/P_{C_3} \sim 10$, whereas for graphite the ratio is 0.17, i.e., the atomic-carbon-enhancement factor is 58.8 for the carbide.

More recent vaporization studies of TaC using laser vaporization mass spectrometry (at 18.6 eV) indicate C_3 as the predominant species [Meyer et al., 1973]. However, the substrate composition is unspecified in these studies and could well be closer to TaC than $TaC_{0.71}$. This situation would tend to favor a higher C_3/C_1 ratio than for the work of Fesenko and Bolgar [1969]. Using the measured relative partial pressures of C_3/C_1, in comparison with values calculated from the Palmer and Shelef [1968] evaluation for graphite, a surface temperature of 4500 K was indicated. The JANAF [1971] derived temperatures would be greater, but vaporization coefficient and

ionization cross section uncertainties probably contribute to this difference. A comparison of the observed TaC and C vapor species abundances (integrated ion intensities) indicates $C_1 : C_2 : C_3$ values of 1.0 : 0.06 : 2.2 and 1.0 : 0.32 : 35, respectively, and presumably at 4500 K in both cases. These observations do not necessarily conflict with the lower temperature studies of Fesenko and Bolgar [1969] owing to the large temperature differences together with the strong C_3/C_1 temperature dependence.

Meyer et al., [1973] argue that the carbide vapor composition may reflect the molecular structure of the solid phase and that different carbides may produce different C_n distributions. A higher laser energy (18 J of focused energy versus 0.1 J for graphite) was needed for TaC due to its greater reflectivity. The results could not be quantified because of the non-congruent vaporization. Also, no direct indication of the TaC temperature was obtained in these experiments, but the signals were approximately an order of magnitude weaker than for graphite.

In view of the incomplete and disparate nature of the literature studies, further examination of the molecular composition in laser plumes over tantalum carbide samples is needed and planned.

3. Subtask B: Cluster Formation Studies

Laser vaporization processes can result in relatively high pressures of vapor species, as shown by the results for C_n given in Section 2. When a high pressure vapor expands adiabatically into a vacuum environment the temperature can fall markedly, leading to a supersaturated vapor state. Such a condition tends to favor homogeneous nucleation, with the formation of cluster intermediate, aerosol, and particulate states. While the laser vaporization studies of graphite, described in Section 2, showed evidence of expansion-cooling there was no indication of cluster formation. Independent

control of the source pressure and temperature, which was not possible with the graphite studies, is required to understand the mechanistic details of the vapor to cluster to aerosol transformation. For this purpose, we have developed a chamber in which the total pressure and temperature can be independently controlled, and from which expansions into a vacuum chamber can be monitored with mass spectrometric detection [Bonnell and Hastie, 1979]. Alkali halides have been selected as test cases for monitoring cluster formation processes.

The apparatus, termed Transpiration Mass Spectrometer (TMS), consists of an initial chamber for vapor transpiration and molecular beam production, and a second chamber where modulation of the molecular beam and mass analysis are performed. Figure 7 shows the transpiration inlet system, located in a vacuum chamber. The entire system is heated by a tantalum foil furnace (not shown), and the beam is directed to a quadrupole mass spectrometer which is operated in a cross-beam configuration. The unit is laser aligned with the beam axis directed toward the ion source. Differentially pumped apertures collimate the beam and a mechanical chopper modulates the beam to allow phase sensitive lock-in amplification. The two-stage vacuum system used is similar in concept to the LIV system (shown in fig. 2) but with a horizontal beam-path geometry.

Vapor expansion experiments were conducted with KCl and NaCl vapor, in a N_2 carrier gas, at source pressures of ~ 0.04 MPa (0.4 atm) and temperatures to 1300 K. The data have been discussed in detail elsewhere [Hastie, et al., 1984], including a complete thermochemical analysis. Studies with variable pressure of nitrogen and orifice size were conducted to identify excess dimer/trimer formation due to possible clustering by expansion cooling. For the smaller orifice, (lower final beam temperature), the ion intensity ratio

of dimer to monomer species decreased with increased N_2 pressure (ie, decreased beam temperature), which indicated an absence of clustering. Similar results were found for the NaCl system.

One possible explanation for these results could be that higher molecular weight clusters fragment, thereby contributing to ion signals for the lower polymers. Our analysis indicates, however, that such effects must be less than about 10 percent, as neither phase (time-of-flight) data nor appearance potentials show any evidence for unexplained contributions to assigned precursors. Similar arguments pertain to the C_n system which also showed no evidence for cluster formation.

4. Subtask C: Results on Ionization Processes

In order to identify gaseous species in complex high temperature vapors, a mass spectrometer must be used to ionize and detect the neutrals. However, the electron impact ionization process frequently produces fragment ions. A universal assumption in high temperature mass spectrometry is that intensity ratios of fragment to parent ion are temperature independent, as might be argued from the thermal energy being negligible with respect to the ionizing energy. One known exception for high temperature species has been reported by Askishin et al., [1960] for the CsCl system, where a 20 percent variation in the ratio $Cs^+/CsCl^+$ was observed over the temperature interval 800 to 900 K. These authors argued that temperature-dependence in the Franck-Condon factors was the result of poor overlap between the ground state of CsCl with the bound ion state. Changes in the thermal population of the higher vibrational states with temperature would then influence the Franck-Condon factors.

A relatively simple model of the temperature-dependent ionization process has been discussed by Dronin and Gorokov [1972], and also Nikolaev [1972]. Figure 8 shows a harmonic oscillator potential model for the ground state, located such that only a small overlap occurs with the stable region ($r > r_c$) of the bound-ion state. The stable region is defined by vertical transitions (the Franck-Condon assumption for electron impact excitation) from the ground state to the ion-state region to the right of the internuclear distance where the ion dissociation limit intersects the ion-state repulsive wall, as shown in figure 8. The population fractions $f_v(T)$ of the various vibrational states can be determined, from which the fragmentation ratio can be calculated using the relationship:

$$R = M^+/MCl^+ = \left(\sum_{v=0}^{\infty} \left[\int_{r_c}^{\infty} \left\{ Y_v^* \, Y_v \, dr \right\} \cdot f_v(T) \right] - 1 \right)^{-1}, \qquad (4.1)$$

where Y_v is the vibrational eigenfunction for vibrational state v. From this expression, transitions from the ground state to the right of r_c lead to parent ion formation, and transitions to the left of r_c produce dissociation to fragments (see fig. 8). Although Nikolaev [1972] presented calculations of r_c, based on a model of the ion-state, he found it necessary to compute r_c for CsCl empirically using the experimental fragmentation ratio. With this approach he obtained $r_c = 0.342$ nm, compared to the calculated value of 0.323 nm.

A more definitive, generally applicable model for this relatively novel process (for high temperature species) has been obtained under the present subtask using the TMS system. The isentropic expansion used to form a representative non-interacting beam from a high temperature region provides extreme rotational and vibrational cooling of the molecules. This cooling

effect has led to observation of anomalously high ratios of M^+/MX^+ in alkali halide species [Bonnell and Hastie, 1983]. The above model provides a basis for interpreting these experimental data since the proper temperature describing molecules in the beam is given by the isentropic temperature of the expansion rather than the source temperature. For suitable orifice dimensions, the temperature can be altered over a wide range by varying the system pressure. At high temperatures, the vibrational levels are significantly populated, up to v = 10 or more. For the NaCl case, considered in detail here, less than half of the molecules at 800 K are in the v = 0 state (harmonic oscillator assumption); one percent, or more, occupancy is found up to the level v = 8. It follows that an empirical interpretation based on the observed high temperature ratio is so insensitive to small changes in the value of r_c that almost no information can be obtained from hot beams.

Figure 9 shows a low temperature ion-ratio limit near R = 27 for the NaCl case (TMS data). For the harmonic oscillator fit, values of ω_e = 363.62 cm^{-1} and r_e = 0.23606 nm were used. Equation 4.1 was evaluated by numerical integration of harmonic oscillator Y_v's and direct summation over v from 0 to 12. The evaluation was iterated on r_c with T = 10 K until the experimental value, R = 27 ± 0.5 was obtained and the corresponding value of r_c was 0.24648 ± 0.0001 nm. Note that the high precision obtained for r_c is indicative of the high sensitivity of this model approach. The temperature-dependence results based on this fit are plotted in figure 9 as the Harmonic Oscillator curve. It is clear that the qualitative shape of the data (including effusive measurements taken from the literature [Bonnell and Hastie, 1979]) is adequately modeled by the harmonic oscillator approximation. But even with a possible error of a factor of two in beam temperature (which has been applied to the data), the model does not quantitatively

fit either the TMS or KMS effusive data. A likely explanation of the model's deficiency is that the ground state well is anharmonic, and the harmonic oscillator eigenvalues of the levels underestimate upper level participation.

The curve labeled High Temp. Fit in figure 9 is based on a harmonic oscillator-model calculation, made using only the high temperature effusion data. Note the disagreement of this model approach with that using the low temperature (EXPANSION) data. This difference indicates the impossibility of successfully modeling temperature dependent fragmentation based only on high temperature data. Also, the extreme sensitivity of the model prediction on the value of r_c is demonstrated by comparison of the high temperature fit and low temperature anharmonic oscillator results, shown in figure 9. This sensitivity indicates that low temperature ion-intensity data can provide a stringent test of ground state potential well shape, particularly for levels above the ground vibrational state.

The basis for the anharmonic model used is as follows. The potential well was computed by the Rydberg-Klein-Rees method from the spectroscopic data selected by JANAF [1971]: ω_e = 363.62, $\omega_e x_e$ = 1.72, B_e = 0.21691, all in cm^{-1}. These values imply r_e = 0.23671 nm. The function, $f_v(T)$ was summed directly from the anharmonic eigenvalues

$$E_v = \omega_e(v + 1/2) - \omega_e x_e(v - 1/2)^2,$$

normalized by summing to v = 15 where the population, even at 1200 K, was insignificant. The anharmonic eigenfunctions were approximated by mapping harmonic oscillator eigenfunctions onto the actual potential well. Figure 9 shows the resulting model behavior for R with T, given as the Anharmonic

Oscillator curve (r_c = 0.2445 ± 0.0001 nm). The model agreement with the TMS data is now excellent; however, the model still fails to predict the effusive KMS data. Possible explanations are:

- o Harmonic oscillator eigenfunctions are not a good model at high temperature--the "true" eigenfunctions do exhibit higher amplitude toward the right wall of an anharmonic potential than toward the left.
- o Centrifugal broadening of the potential-well and high rotational level occupation may be important in the calculation--at T > 800 K, J(max) is of the order of 60; the effect on $f_v(T)$ and Y_v may be more significant than the effect on the potential well.
- o Avoided-crossing distortions of the potential-well may be important at high temperatures although Oppenheimer and Berry [1971] calculate that point for NaCl to be at r = 0.94 nm, where no significant thermal occupation would exist.
- o The actual form of the potential may not be accurate enough above v = 2-3.
- o The separation of the two states of the ion, expected to exist, may cause the simple overlap model to fail at higher temperatures.

An abinitio calculation for this problem is now possible and probably warranted. However, many important systems are not yet calculable, and fragmentation at a single bond is a very important case. The sensitivity shown by this model also points to the possibility of directly using this effect to test existing abinitio calculations of the higher energy levels.

5.0 References

Akishin, P. A., Gorokov, L. N., and Sidorov, L. N. [1960]. Proc. Acad. Sci. USSR. (Dok. Phys. Chem.) 135, 1001.

Baker, R. L., Covington, M.A., and Rosenblatt, G. M. [1983]. "The Determination of Carbon Thermochemical Properties by Laser Vaporization". P. 143 in High Temperature Materials Chemistry, Eds. Munir, Z. A., and Cubicciotti, D., Electrochem. Soc., Pennington, NJ.

Berkowitz, J., and Chupka, W. [1964]. J. Chem. Phys. 40, 2735.

Bonnell, D. W., and Hastie, J. W. [1979]. P. 357 in Characterization of High Temperature Vapors and Gases, J. W. Hastie, ed., NBS SP 561, U.S. Govt. Printing Office, Washington, DC.

Bonnell, D. W., and Hastie, J. W. [1983]. A Theoretical Analysis of Temperature Dependent Electron Impact Fragmentation, 31st Ann. Meeting, Amer. Soc. Mass Spec., Boston.

Clarke, J. J., and Fox, B. R. [1969]. J. Chem. Phys. 51, 3231.

Covington, M. A., Liu, G. N., and Lincoln, K. A. [1977]. AIAA J. 15, 1174.

Dronin, A. A., and Gorokov, L. N. [1972]. Teplofiz. Vys. Temp. 10, 49.

Drowart, J., Burns, R. P., De Maria, G., and Inghram, M. G. [1959]. J. Chem. Phys. 31, 1131.

Fesenko, V. V., and Bolgar, A. S. [1969]. Teplofiz. Vys. Temp. 7, 244.

Gupta, S. K., and Gingerich, K. A. [1979]. J. Chem. Phys. 71, 3072.

Hall, R. [1984] Private Communication.

Hastie, J. W., Zmbov, K. F., and Bonnell, D. W., [1984]. "Transpiration Mass Spectrometric Analysis of Liquid KCl and KOH Vaporization," High Temp. Science, in press.

"JANAF Thermochemical Tables", 2nd ed., NSRDS-NBS 37 (Washington, DC, 1971).

Leider, H. R., Krikorian, O. H., and Young, D. A. [1973]. Carbon 11, 555.

Lincoln, K. A. [1969]. P. 323 in "High Temperature Technology," Butterworths and Co., London.

Lincoln, K. A., and Covington, M. A. [1975]. Int. J. Mass Spec. Ion Phys. 16, 191.

Lundell, J. H., and Dickey, R. R. [1977]. Progr. Astron. and Aeron. 56, 405.

Lundell, J. H. [1982]. Progr. Astron. and Aeron. 83, 472.

Meyer, R. T., and Lynch, A. W. [1973]. High Temp. Science 5, 192.

Meyer, R. T., Lynch, A. W., and Freese, J. M. [1973]. J. Phys. Chem. 77, 1083.

Milne, T. A., Beachey, J. E., and Greene, F. T. [1972]. In "Vaporization Kinetics and Thermodynamics of Graphite Using the High Pressure Mass Spectrometer," AFML-TR-72-227 (AD 753713).

Nikolaev, E. N. [1972]. Khim. Vys. Energii, 3, 49.

Ohse, R. W., Babelot, J. F., Cercignani, C., Kinsman, P. J., Long, K. A., Magill, J., and Scotti, A., [1979]. P. 83 in Characterization of High Temperature Vapors and Gases, J. W. Hastie, ed., NBS SP 561, U.S. Govt. Printing Office, Washington, DC.

Olstad, R. A., and Olander, D. R. [1975]. J. Appl. Phys. 46, 1509.

Oppenheimer, M., and Berry, R. S. [1971]. J. Chem. Phys., 54, 5058.

Palmer, H. B., and Shelef, M. [1968]. Carbon 4, 85.

Sterns, C. A., Kohl, F. J., Fryburg, G. C., and Miller [1979]. P. 303 in Characterization of High Temperature Vapors and Gases, J. W. Hastie, ed., NBS SP 561, U. S. Govt. Printing Office, Washington, DC

Strauss, H. L., and Thiele, E. [1967]. J. Chem. Phys., 46, 2473.

Thorn, R. J., and Winslow, G. H. [1957]. J. Chem. Phys. 26, 186.

Wachi, F. M., and Gilmartin, D. E. [1970]. Carbon 8, 141.

Wulfson, E.K., Dworkin, W.I., and Karjakin, A. W. [1980]. Spectrochim. Acta 35B, 11.

Zavitsanos, P. D., [1968]. Carbon 6, 731.

Zavitsanos, P. D., and Carlson, G. A. [1973]. J. Chem. Phys. 59, 2966.

Table 1. C_n Ion Intensities and Corresponding Calculated Equilibrium Surface Temperatures[a]

Mass (amu)	Species	Peak Signal	Integrated Signal	Temperature (K)[b]
		Ionizing electron energy = 96 eV		
12	C_1	0.51	0.32	2600
24	C_2	0.16	0.12	3450
36	C_3	1.0	1.0	---
48	C_4	0.015	0.018	4400
50	C_5	0.04	0.04	4300
		Ionizing electron energy = 26 eV		
12	C_1	0.47	0.32	2600
24	C_2	0.14	0.11	3200
36	C_3	1.0	1.0	---
48	C_4	0.014	0.013	4100
50	C_5	0.027	0.027	4000

[a]The accuracy of the C_1 and C_2 ratios to C_3 is about 30 and 10 percent, respectively; for C_4 and C_5 the accuracy is about 25 percent. Typical C_3 signals are 100 to 200 mv peak.

[b]Obtained by comparison of observed Integrated Signal intensities, relative to C_3, with the JANAF [1971] thermochemical partial pressure data.

Table 2. Surface Temperature Results in the Graphite System

Method	Temperature (K)
C_2^+ arrival time relative to B^+ (at 2900 K)	4000 ± 300
P_C from $P = k\, I(C^+)\, T$, with JANAF [1971]	4200 ± 300
C^+/B^+ intensity ratio (for B at 2900 K)	4100 ± 300
C_4 (or C_5)/C_3, with JANAF [1971]	4100 ± 300
Average	4100 ± (300)

Table 3. Comparison of Present Results with Zavitsanos [1968] Ion Intensities, Normalized to C_3 at 4100 K

Ion	Zavitsanos (20 eV)	This Work (26 eV)
C_1	0.48	0.47
C_2	1.00	0.14
C_3	1.00	1.0
C_4	0.24	0.014
C_5	0.39	0.027
C_6	0.15	<0.01
C_7	0.16	---

Table 4. Comparison of Present Ion Intensity Results with the Milne et al., [1972] Extrapolated Ion Ratios at 4200 K, Normalized to C_3

	JANAF [1971] Pressure (atm)	Milne, et al. [1972]	This Work (26eV)
C_3	2.5	1.0	1.0
C_1	0.2	0.08 (= JANAF)	0.32
C_2	0.3	0.12 (= JANAF)	0.11
C_4	0.3	0.12	0.013
C_5	0.3	0.12	0.027
C_6 - C_7	0.001	0.0004	<0.01

Table 5. Temperatures Calculated from Partial Pressure Ratios, Relative to C_3

Species	Ion Intensities [This Work, 96 eV]	Temp. K [JANAF]	Relative Pressures [Meyer and Lynch]	Temp. K [Meyer and Lynch]
C_1	0.32	2600	0.1	>5000
C_2	0.12	3450	0.13	3500
C_3	1.0	---	1.0	---
C_4	0.018	4400	0.046	>5000
C_5	0.04	4300	0.094	>5000

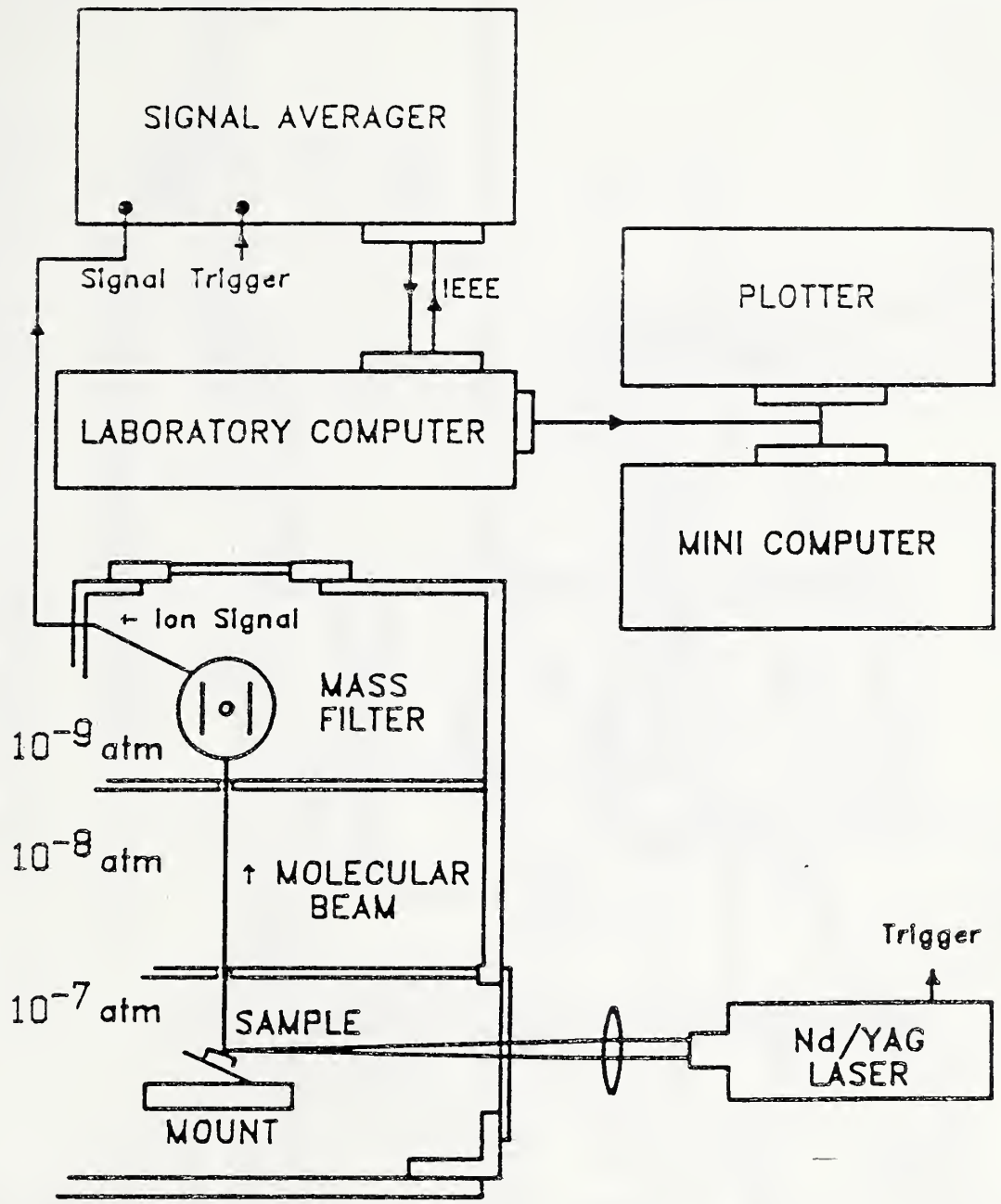

Figure 1. Schematic of laser-induced vaporization mass spectrometric facility (side view), showing laser-sample-molecular beam geometries. The microcomputer system shown controls the signal averager and records completed scans.

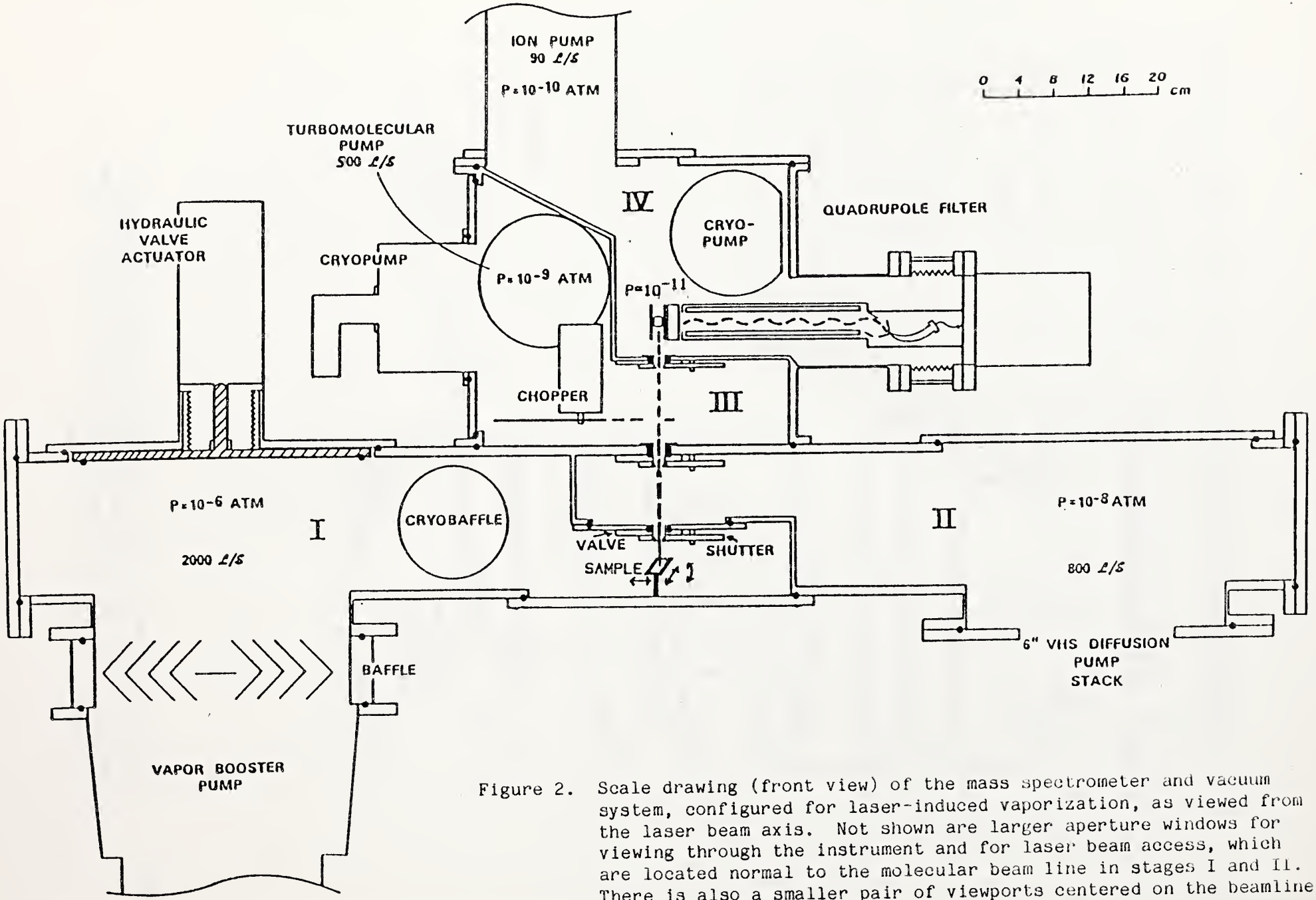

Figure 2. Scale drawing (front view) of the mass spectrometer and vacuum system, configured for laser-induced vaporization, as viewed from the laser beam axis. Not shown are larger aperture windows for viewing through the instrument and for laser beam access, which are located normal to the molecular beam line in stages I and II. There is also a smaller pair of viewports centered on the beamline at the mass spectrometer ion source level (stage IV).

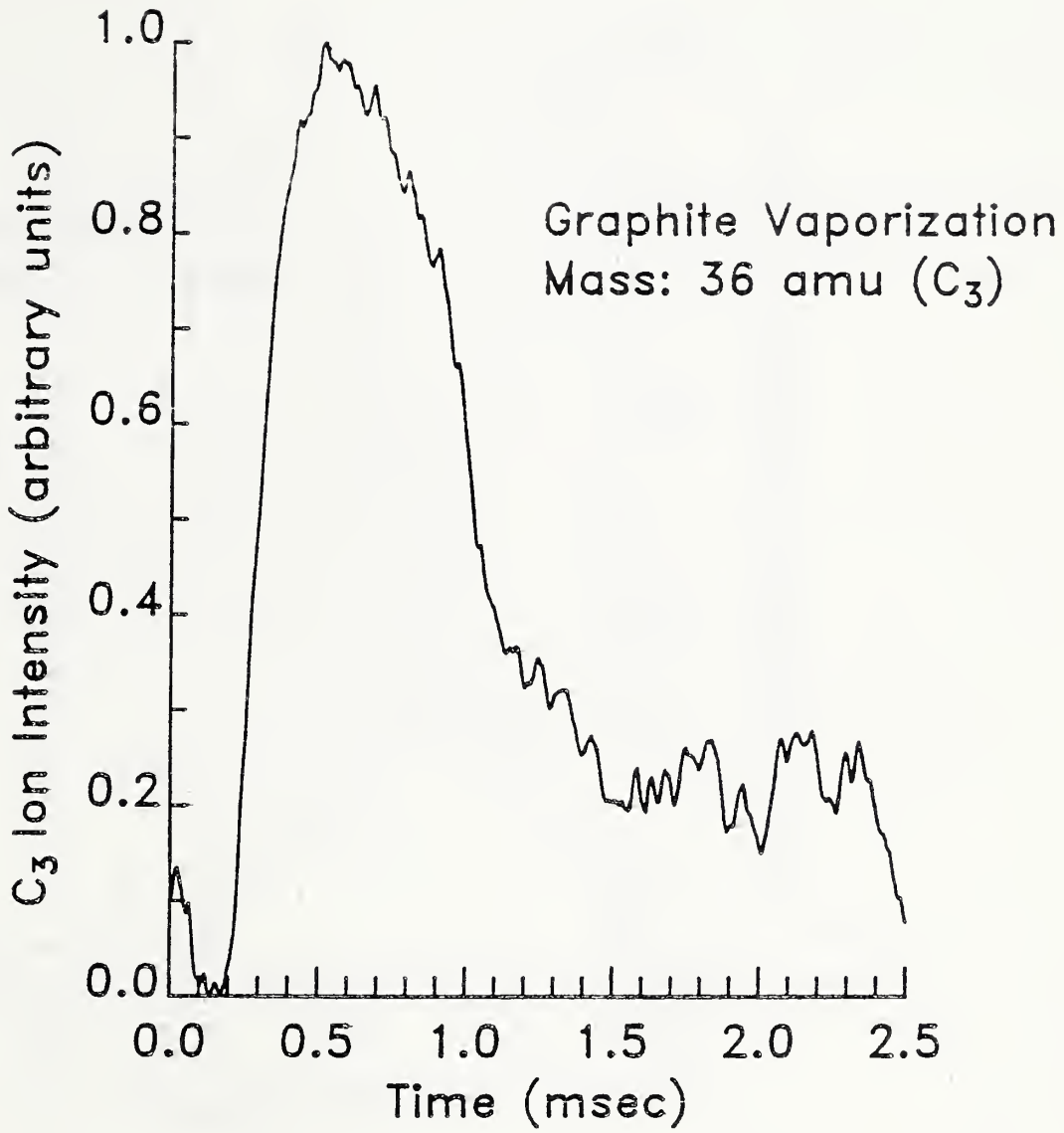

Figure 3. Mass spectral ion intensity-versus-time profile for the 36 amu (C_3^+) ion at 30 eV nominal (26 eV actual) ionizing electron energy. Unit peak-ion-intensity equals 27336 counts.

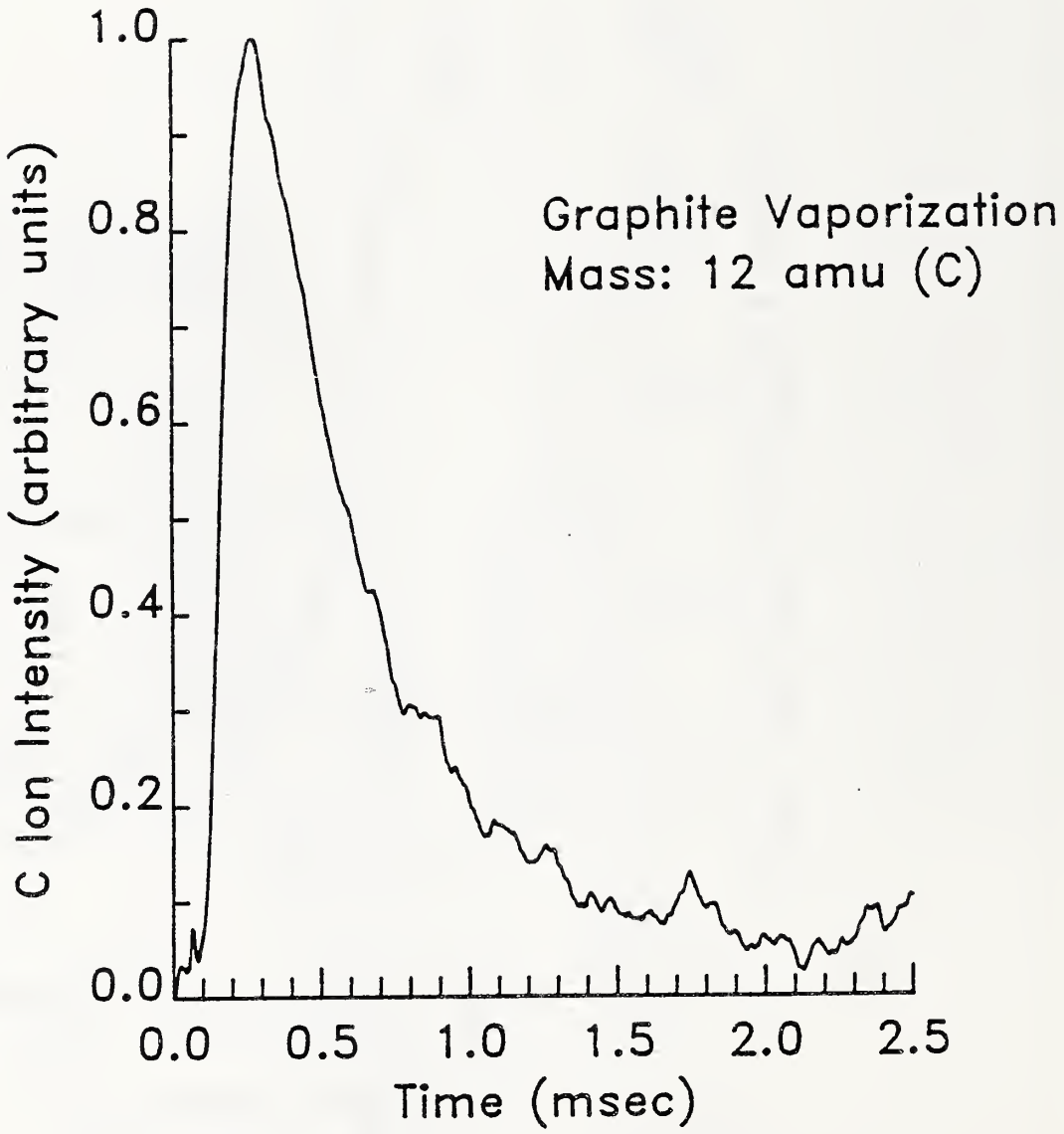

Figure 4. Mass spectral ion intensity-versus-time profile for the 12 amu (C_1^+) ion at 30 eV nominal (26 eV actual) ionizing electron energy. Unit peak-ion-intensity equals 30551 counts.

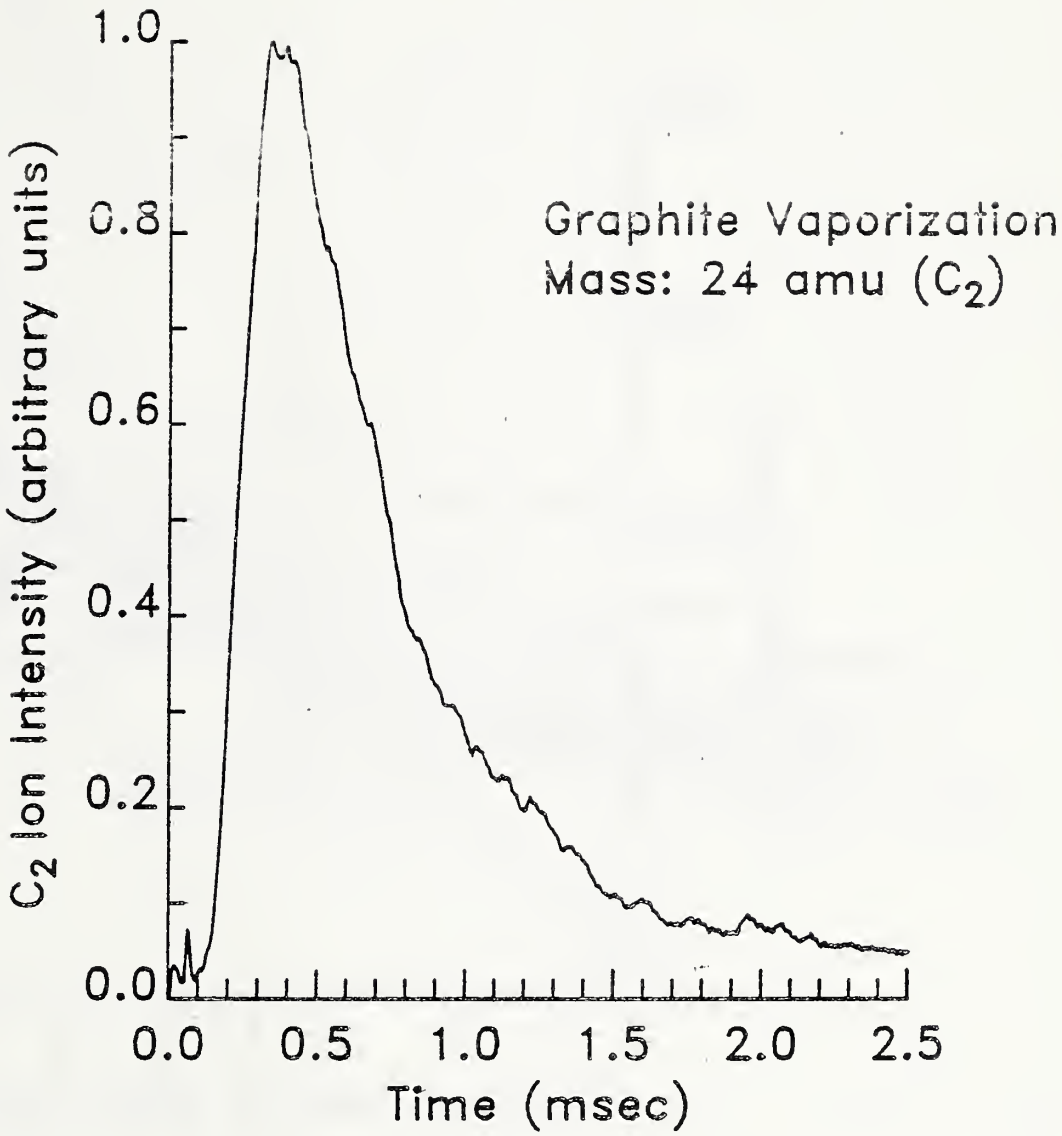

Figure 5. Mass spectral ion intensity-versus-time profile for the 24 amu (C_2^+) ion at 30 eV nominal (26 eV actual) ionizing electron energy. Unit peak-ion-intensity equals 20337 counts.

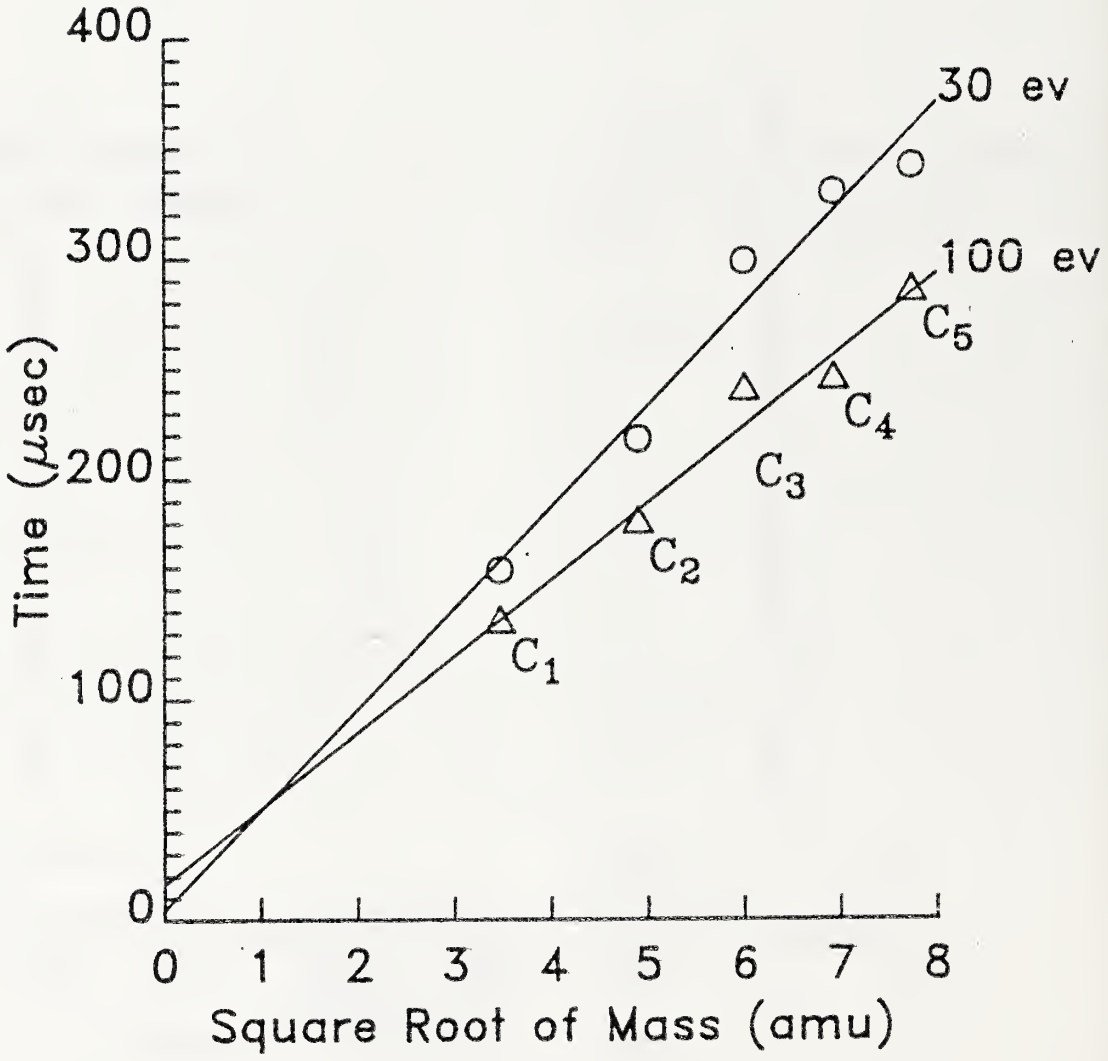

Figure 6. Dependence of the time-of-arrival for C_n^+ (n = 1 to 5) ions as a function of molecular weight from laser vaporized graphite. The linear dependence confirms the assignment of neutral precursors, and indicates a common thermal source and local thermal equilibrium. The two curves shown are for 30 eV and 100 eV nominal ionizing electron energy data sets.

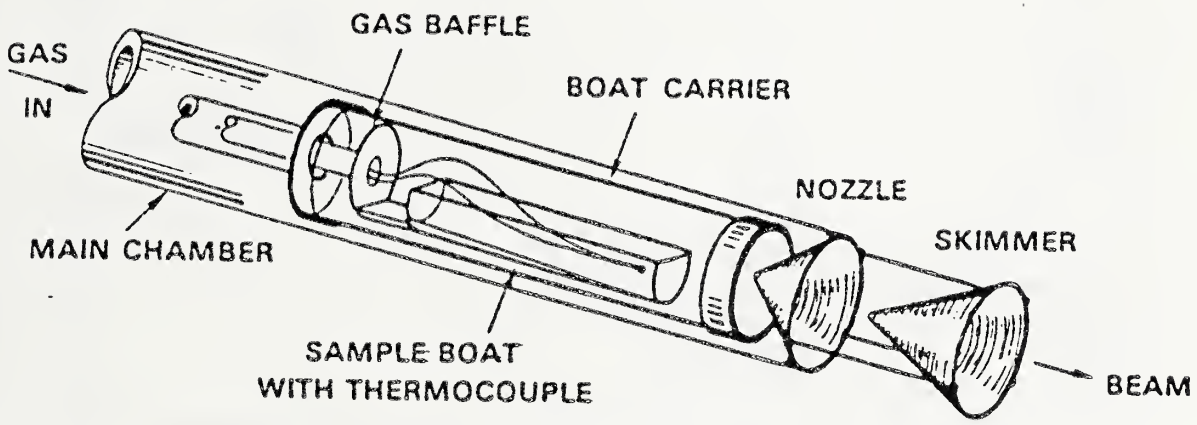

Figure 7. The Transpiration Mass Spectrometer Inlet System.

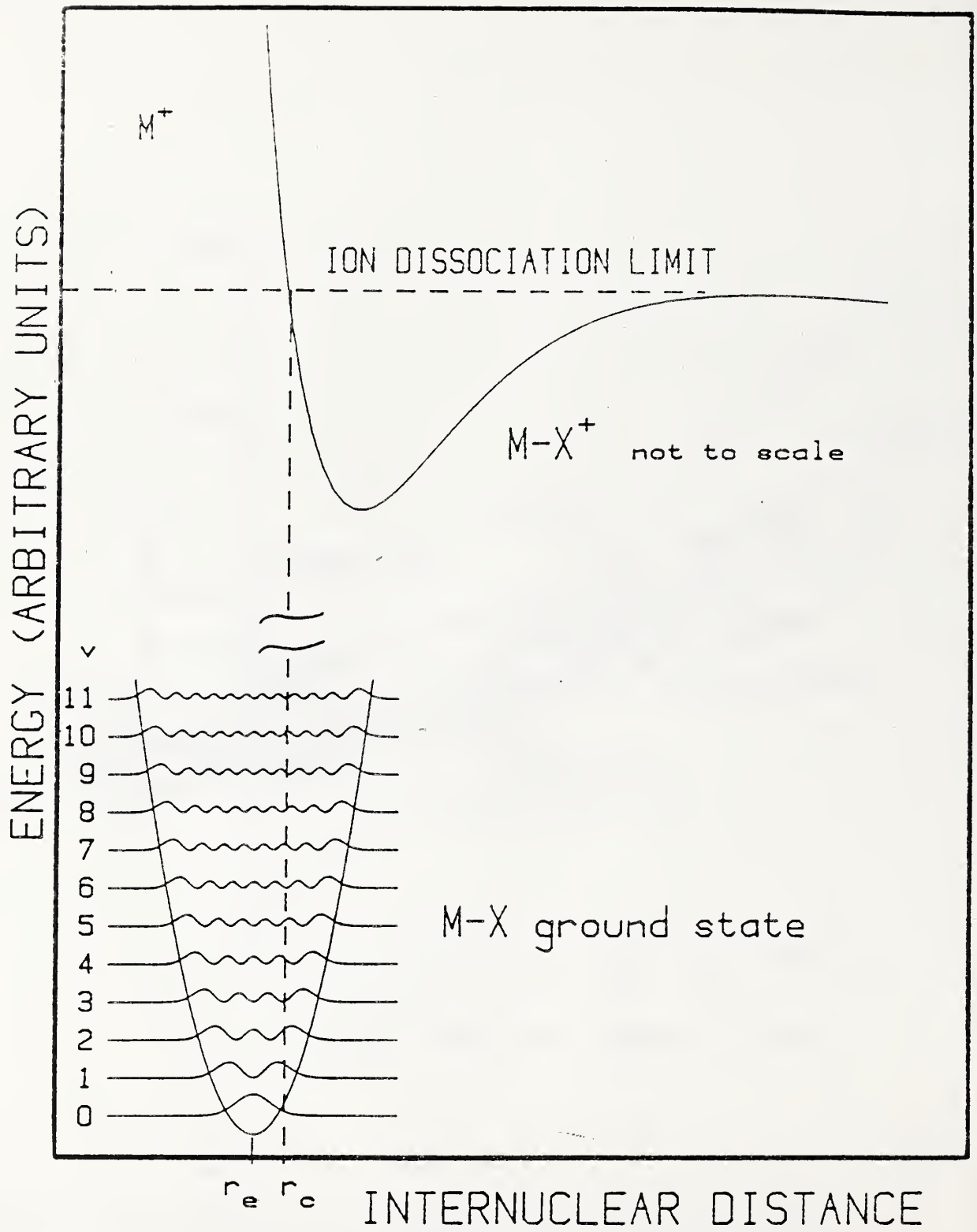

Figure 8. Temperature-dependent electron impact fragmentation model. The lower potential well is for a harmonic oscillator with the probability density functions (square of harmonic oscillator eigen-functions) drawn to scale; r_e is the equilibrium internuclear distance, and r_c represents the dividing line between vertical (Franck-Condon) transitions to a bound molecular ion (at $r > r_c$) and to an unstable condition (at $r < r_c$) giving fragmentation.

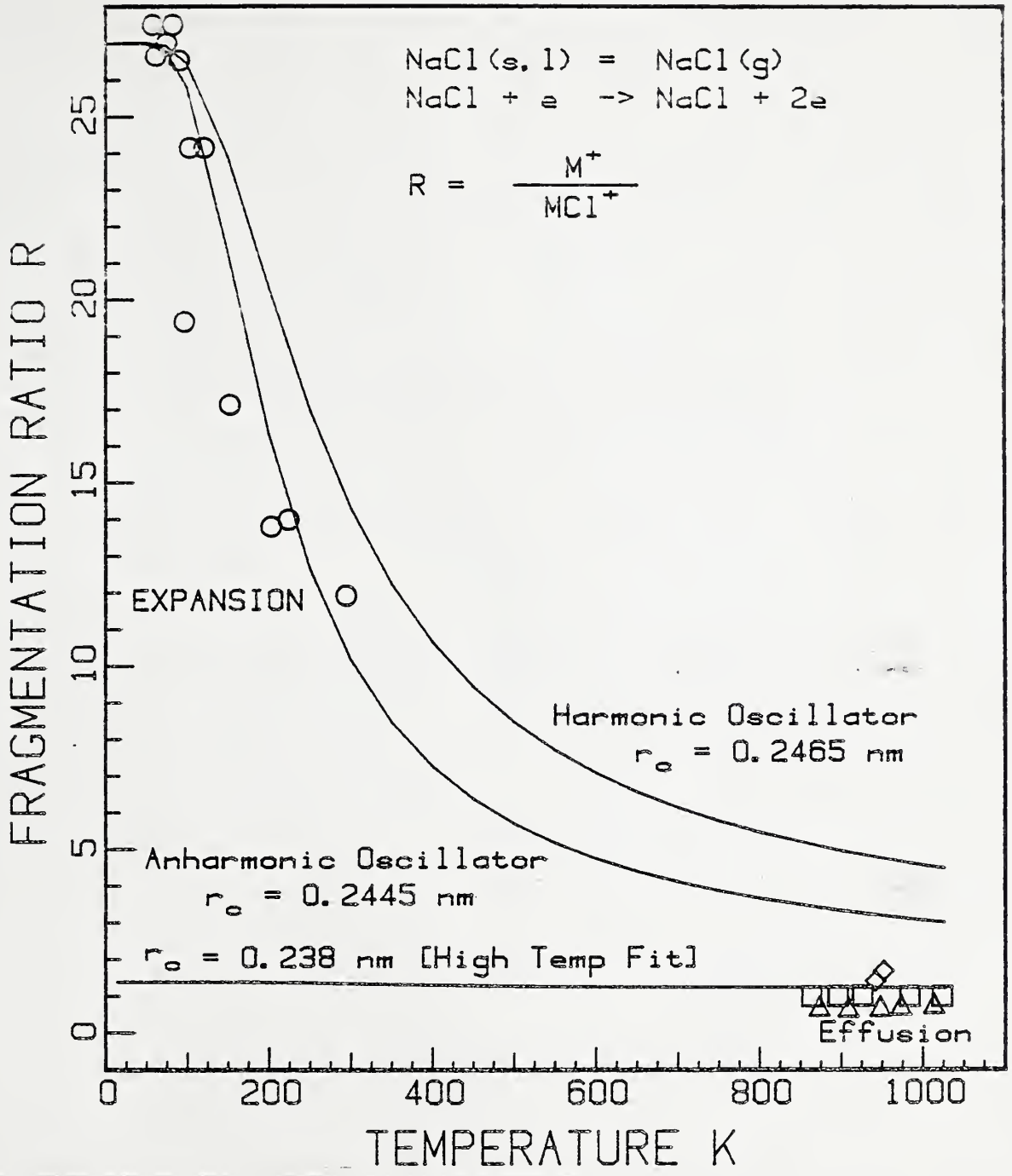

Figure 9. Comparison of experimental and model fragmentation ratios in high pressure expansions of NaCl vapor-N_2 gas mixtures. The temperature axis was derived from the source pressure using an isentropic expansion/sudden-freeze model (see for instance, Stearns, et al., 1979). An expansion effectiveness parameter of 0.5 has been applied to the derived T/T_o. The r_e value labeled High Temp. Fit is for a harmonic oscillator calculation, using only experimental high temperature R-data (see text).

NBS-114A (REV. 2-8C)

U.S. DEPT. OF COMM. BIBLIOGRAPHIC DATA SHEET (See instructions)	1. PUBLICATION OR REPORT NO. NBSIR 84-2983	2. Performing Organ. Report No.	3. Publication Date December 1984

4. TITLE AND SUBTITLE

Molecular Basis for Laser-Induced Vaporization of Refractory Materials

5. AUTHOR(S)
J. W. Hastie, D. W. Bonnell, and P. K. Schenck

6. PERFORMING ORGANIZATION (If joint or other than NBS, see instructions)

NATIONAL BUREAU OF STANDARDS
DEPARTMENT OF COMMERCE
WASHINGTON, D.C. 20234

7. Contract/Grant No.
AFOSR-ISSA-84-00033

8. Type of Report & Period Covered
Annual FY84

9. SPONSORING ORGANIZATION NAME AND COMPLETE ADDRESS (Street, City, State, ZIP)
AFOSR/NE
Electronic & Material Science Directorate
Bolling AFB
Washington, DC 20332

10. SUPPLEMENTARY NOTES

☐ Document describes a computer program; SF-185, FIPS Software Summary, is attached.

11. ABSTRACT (A 200-word or less factual summary of most significant information. If document includes a significant bibliography or literature survey, mention it here)

A new technique has been developed for time-resolved Laser Induced Vaporization (LIV) studies of refractory materials. The apparatus consists of a high power 10 Hz, pulsed Nd/YAG laser coupled to a specially designed high pressure sampling mass spectrometer. Initial studies on an ultra-pure spectroscopic grade graphite sample provided time-resolved quantitative mass spectral peaks, corresponding to C_n (n = 1 -5) molecular species, with excellent signal-to-noise and reproducibility. The absolute and relative intensities of these species were consistent with the establishment of thermodynamic equilibrium at the sample surface. A beam-velocity analysis of the C_n species indicated an appreciable cooling effect in the vapor plume by an adiabatic expansion process. In a separate study, attempts to produce molecular clusters by non-equilibrium adiabatic expansion of NaCl, KCl, and C_n ($n \leq 5$) molecular species showed no evidence of clustering at source vapor pressures to one atmosphere. This result sets limits on the expansion times, source pressure, and temperature conditions needed to produce cluster species for these systems. We have also found that relative ionization cross-sections (σ) can vary quite significantly with temperature, particularly for species exhibiting a large geometry change on ionization. Data obtained for the test systems, NaCl and KCl, exhibited large changes in σ (25:1) between high temperature (~ 1000 K) species and translationally cooled low temperature (~ 50 K) molecules. The results are quantitatively explained by a potential energy curve model.

12. KEY WORDS (Six to twelve entries; alphabetical order; capitalize only proper names; and separate key words by semicolons)
anharmonic, beam velocity, electron impact ionization cross-sections, expansion cooling, graphite, high temperature, laser heating, mass spectrometry, oscillator model, supersonic molecular beam, temperature dependent fragmentation, vaporization

13. AVAILABILITY

☒ Unlimited
☐ For Official Distribution. Do Not Release to NTIS
☐ Order From Superintendent of Documents, U.S. Government Printing Office, Washington, D.C. 20402.
☒ Order From National Technical Information Service (NTIS), Springfield, VA. 22161

14. NO. OF PRINTED PAGES
48

15. Price
$8.50